Acta Crystallographica Section D
Biological Crystallography
ISSN 0907-4449

Inhibitor binding at the protein interface in crystals of a HIV-1 protease complex

Jiří Brynda,[a]* Pavlína Řezáčová,[a] Milan Fábry,[a] Magdalena Hořejší,[a] Renata Štouračová,[a] Milan Souček,[b] Martin Hradílek,[b] Jan Konvalinka[b] and Juraj Sedláček[a]

[a]Institute of Molecular Genetics, Academy of Sciences of the Czech Republic, Flemingovo nám. 2, 16637 Praha 6, Czech Republic, and [b]Institute of Organic Chemistry and Biochemistry, Academy of Sciences of the Czech Republic, Flemingovo nám. 2, 16610 Praha 6, Czech Republic

Correspondence e-mail: brynda@img.cas.cz

Received 3 May 2004
Accepted 1 September 2004

PDB Reference: HIV-1 protease–phenylnorstatine inhibitor complex, 1u8g, r1u8gsf.

Depending on the excess of ligand used for complex formation, the HIV-1 protease complexed with a novel phenylnorstatine inhibitor forms crystals of either hexagonal ($P6_1$) or orthorhombic ($P2_12_12_1$) symmetry. The orthorhombic form shows an unusual complexity of crystal packing: in addition to one inhibitor molecule that is bound to the enzyme active site, the second inhibitor molecule is bound as an outer ligand at the protein interface. Binding of the outer ligand apparently increases the crystal-quality parameters so that the diffraction data allow solution of the structure of the complex at 1.03 Å, the best resolution reported to date. The outer ligand interacts with all four surrounding HIV-1 protease molecules and has a bent conformation owing to its accommodation in the intermolecular space. The parameters of the solved structures of the orthorhombic and hexagonal forms are compared.

1. Introduction

The retroviral protease of HIV (HIV PR) is an enzyme that has been extensively studied by protein crystallography methods (reviewed, for example, in Wlodawer & Vondrasek, 1998). Structure-based drug design then yielded eight drugs that have now been approved for clinical anti-AIDS use (for a review, see Wlodawer & Vondrasek, 1998). The search for novel compounds that would overcome known drug resistance (Erickson & Burt, 1996) has included a combinatorial approach in which large sets of potential inhibitors are screened against resistant HIV PR species as primary targets (Houghten *et al.*, 1991). Using combinatorial peptide libraries, we have already identified several compounds that have good (subnanomolar) inhibitory capacity towards representative drug-resistant HIV PR forms (Rinnova *et al.*, 2000). The phenylnorstatine group, an atypical inhibitor moiety, served the purpose of investigating the potential of replacement of the peptide bond with larger groups. In the previous paper (Brynda *et al.*, 2004) and in the present paper, the structure of wild-type HIV-1 PR complexed with one of these inhibitors, Z-Pns-Phe-Glu-Glu-NH_2 [Z, benzyloxycarbonyl; Pns, phenylnorstatine, (2*RS*,3*S*)-3-amino-2-hydroxy-4-phenylbutanoic acid] is described. Using a sixfold molar excess of ligand for pre-forming the HIV-1 PR complex, the protein–inhibitor crystals grew to an extraordinary diffraction quality, allowing thus the structure to be determined at 1.03 Å resolution; to our knowledge, this is the highest resolution of any HIV PR–inhibitor complex reported to date (PDB as of June 2004).

Table 1
X-ray data-collection and processing statistics.

Values in parentheses correspond to the last resolution shell.

Space group	$P2_12_12_1$	$P6_1$
Unit-cell parameters (Å)	a = 28.85, b = 66.52, c = 93.10	a = 61.37, b = 61.37, c = 80.52
Diffraction limits (Å)	54.1–1.03 (1.06–1.03)	26.54–2.20 (2.33–2.20)
No. measured diffraction maxima	872620	54226
No. unique reflections	88784	8742
Average $I/\sigma(I)$	10.5 (1.85)	10.4 (2.56)
R_{sym} (%)	7.8 (37.9)	11.3 (58.7)
Completeness (%)	99.0 (93.3)	99.3 (97.1)
Wilson B factor (Å^2)	7.9	46.9

Table 2
Refinement statistics.

Space group	$P2_12_12_1$	$P6_1$
R factor (%)	13.0	20.9
R_{free} factor (%)	16.5	26.3
Non-H atoms in model	1937	1669
Water molecules	233	17
Reflections used in refinement	86020	8326
Reflections in test set	2205	413
Rm.s.d. from ideal bond distances (Å)	0.016	0.17
R.m.s.d. from ideal valence-angle values (°)	0.036 Å†	2.94
Program used	*SHELX*97	*REFMAC* 5.1.24

† Distance between two atoms that are both bonded to the same atom.

2. Experimental

2.1. Crystallization

The inhibitor Z-Pns-Phe-Glu-Glu-NH_2 belongs to a series of inhibitors that replace the scissile bond at the cleavage site of the substrate with a phenylnorstatine group. The inhibitor was synthesized on Rink amide MBHA resin using the Fmoc/*t*-butyl-HOBt/DIC strategy, as published previously (Rinnova *et al.*, 2000). HIV-1 PR (wild type, Bru isolate) used for complex formation and crystallization was obtained by recombinant expression as described previously (Sedlacek *et al.*, 1993).

In trials using the hanging-drop technique, hexagonal as well as orthorhombic crystals were obtained with buffer containing 50 m*M* MES pH 6.5, 2.4 *M* ammonium sulfate as the precipitating agent. The procedure comprised pre-formation of the complex using a sixfold molar excess of inhibitor in the case of orthorhombic crystals and a threefold to fourfold molar excess of the inhibitor in the case of hexagonal crystals. The complex solution containing 10 m*M* sodium acetate pH 5.6, 0.05%(*v*/*v*) 2-mercaptoethanol, 1 m*M* ethylenediaminetetraacetic acid (EDTA) was concentrated to 2.2 mg ml^{-1} protease in a Centricon-10 (Millipore) cell. Each hanging drop consisted of 2 µl concentrated complex solution and 1 µl reservoir solution. Hexagonal crystals appeared overnight, whereas orthorhombic crystals appeared after several days of equilibration at 291 K. Crystals were mounted in a nylon loop, soaked in cryoprotectant solution [reservoir solution with 20%(*v*/*v*) glycerol] for a few seconds, bathed in paraffin oil and finally transferred into liquid nitrogen and stored frozen.

2.2. X-ray data collection, structure determination and analysis

Data collection from orthorhombic crystals and determination and refinement of the orthorhombic structure are described in detail in Brynda *et al.* (2004). Coordinates and structure factors for this structure have been deposited with PDB code 1nh0.

The best hexagonal crystal, with dimensions 0.08 × 0.08 × 0.5 mm, was used for measurements. Diffraction data were collected on beamline ID14-2 at the European Synchrotron Radiation Facility, Grenoble at 0.93 Å wavelength, using an ADSC Q4 CCD-based detector at 100 K (Oxford Cryosystems). The data were integrated using *XDS* (Kabsch, 2001*a*) and scaled using *XSCALE* (Kabsch, 2001*b*), *i.e.* by the same procedure as described for the orthorhombic crystals (Brynda *et al.*, 2004). Table 1 summarizes the data-collection statistics.

Since our hexagonal crystal appeared to be isomorphous with all other $P6_1$ crystals of HIV-1 protease complexes, structure determination was performed by the rigid-body refinement protocol using 1vij as the initial model and then by the restrained refinement protocol, both using *REFMAC* v.5.1.24 (Collaborative Computational Project, Number 4, 1994). At this point, the inhibitor was built in the active site according to the difference electron-density map ($m|F_o| - D|F_c|$ coefficients) and its known position in the orthorhombic structure using *XtalView* (McRee, 1999). After a few cycles of restrained refinement, water molecules were added and the model was again refined using *REFMAC*. Coordinates and structure factors for this hexagonal structure have been deposited as PDB code 1u8g. The final refinement statistics are summarized in Table 2.

Analysis of crystal contacts was performed using *CONTACT* (Collaborative Computational Project, Number 4, 1994). The parameters for contact counts were as follows: hydrogen-bond distance limits were 2.25–3.25 Å (non-H–non-H atom) and the van der Waals bond distance limit was 3.9 Å (non-H–non-H atom). The molecular models used comprised only protein and inhibitor molecules; water, ions and other small molecules were ignored. In the cases of dual conformations, the atoms having partial occupancy were counted with their respective occupancy factors.

Density of crystal packing is expressed as the volume of the unit cell divided by the number of liganded HIV PR dimers in it; this (reciprocal) parameter is termed 'per HIV PR molecule volume'. The solvent contents were calculated with *MATTHEWS_COEF* program (Collaborative Computational Project, Number 4, 1994).

3. Results

3.1. Resolution limit and model quality

The three-dimensional structure of HIV-1 protease complexed with a recently characterized inhibitor (Rinnova *et al.*, 2000), Z-Pns-Phe-Glu-Glu-NH_2 (see §1 for abbreviations and Fig. 1 for the formula) was determined (see also Brynda *et al.*, 2004). Orthorhombic crystals grown from a co-crystal-

lization mixture containing a sixfold molar excess of the inhibitor (see §2) diffracted to nearly 1 Å resolution. For the chosen resolution of 1.03 Å, reflections in the last shell had an average $I/\sigma(I)$ ratio of higher than 1.85. After molecular replacement and rigid-body refinement, electron density for the inhibitor molecule in the active site was clearly recognizable. On the basis of additional continuous positive electron density in the solvent region, the second molecule of the inhibitor bound to the outer protein surface was built into the model (Fig. 2). Although the compound used for complex formation and crystal growth had mixed *R* and *S* chirality at the C21 C atom (the only racemic atom), both bound inhibitor molecules were of *R* chirality at C21.

Remarkably, co-crystallization from a mixture having the same composition except for a lower (threefold) molar excess of the inhibitor led to the growth of hexagonal crystals (space group $P6_1$) that diffracted to 2.2 Å resolution (PDB code 1u8g). Table 2 summarizes the data-collection, processing and structure-refinement statistics. In brief, a single inhibitor molecule was found in the active site with a mixed orientation, as consistently observed with all other hexagonal crystals (*e.g.* Dohnálek *et al.*, 2001). The inhibitor structure is identical to that of the active-site inhibitor molecule in the $P2_12_12_1$ form: the r.m.s.d.s for the two orientations in the $P6_1$ form are 0.101 and 0.109 Å, respectively, calculated against all 53 non-H atoms of the prevalent conformation of the active-site inhibitor of the $P2_12_12_1$ form.

The final map obtained for the orthorhombic form showed very clear electron densities for all side chains except for those of two HIV PR surface amino-acid residues, LysA14 and ArgA41. The refined model contains 198 amino acids, two inhibitor molecules, 230 water molecules, two sulfate anions, a complete mercaptoethanol molecule bound to residue CysA67 and another mercaptoethanol molecule represented only by its S atom at a distinctive covalent-binding distance to atom SG of CysB67, similar to that of other PDB entries (*e.g.* 1dif, 1hih). The model of the protease has 94.9% of the non-glycine and non-proline residues in the most favoured region of the Ramachandran plot and the remainder in the additionally allowed region. Remarkably, the model accuracy of the atom coordinates and their statistical deviations permits an assessment of the protonation/deprotonation of carboxylic O atoms of the enzyme catalytic aspartates on the basis of C—O distances (Wlodawer *et al.*, 2001), as detailed elsewhere (Brynda *et al.*, 2004).

3.2. Crystal packing: contacts of the inhibitor with outer protein surface

The complex crystallized in space group $P2_12_12_1$ and the asymmetric part of the unit cell contained one molecule of HIV PR dimer and two molecules of the inhibitor, one in the active site and one as an outer ligand (Fig. 3). The arrangement of the protein molecules in the crystal lattice is distinctly different from that commonly found in other $P2_12_12_1$ orthorhombic crystals of HIV PR complexes (March *et al.*, 1996; Prabu-Jeyabalan *et al.*, 2000; Mahalingam *et al.*, 2001, 2002; King *et al.*, 2002). As shown in Fig. 3 (see also the stereoview in Fig. 4*b*), the orientation of the protein molecules is basically such that a region to the 'left' of the four-termini region of a HIV PR molecule points towards one arm of the flap structure of one neighbouring HIV PR molecule, while the region to the 'right' of the four-termini region points towards one arm of the flap structure of another neighbouring HIV PR molecule. Each HIV PR has one inhibitor molecule in its active site and the additional inhibitor molecules consistently occupy the sites where the flap and the four-termini regions of HIV PR molecules are close to each other in the crystal lattice.

Each molecule of the inhibitor bound to the outer protein surfaces makes intermolecular contacts with the protein chains of four HIV PR molecules. The outer ligand inhibitor molecule has a bent conformation, in contrast to the extended conformation of the inhibitor molecule bound to the active site; a more detailed comparison is given in the following section. The outer ligand interacts *via* two hydrogen bonds with two amino-acid residues in the terminal region of one HIV PR molecule (J1 O9 to TrpA6 NE1 and GluJ4 OE1 to ThrA4 OG1) and *via* one hydrogen bond to a symmetry-related HIV PR molecule (GluJ4 NXT to CysB67 O).

The outer ligand makes one hydrogen bond to the N-terminal region of one HIV PR molecule (J1 O9 to TrpA6 NE1, 2.91 Å). The outer ligand displays a number of

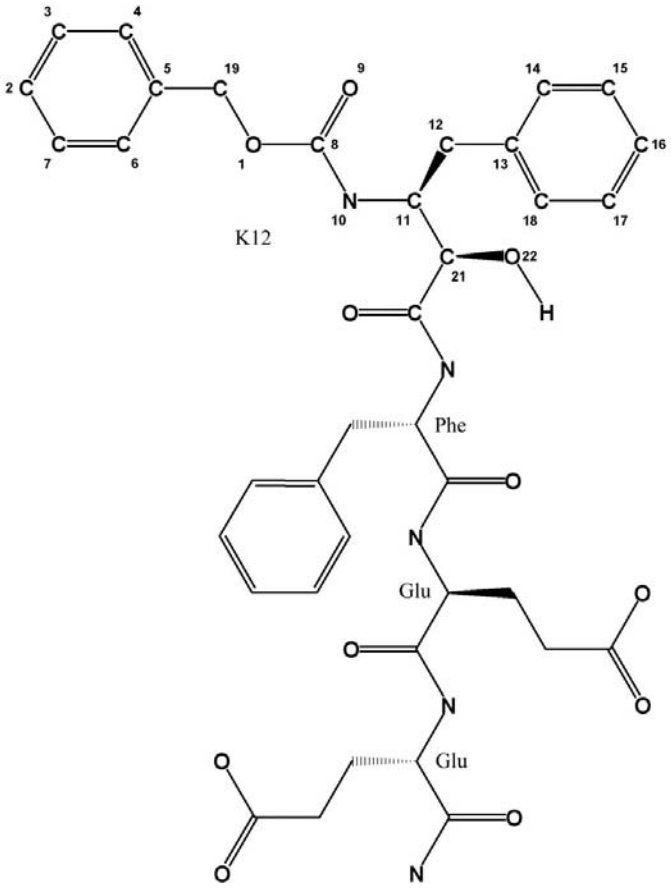

Figure 1
Chemical structure of the inhibitor; the numbering of atoms and labelling of residues correspond to the deposited PDB file.

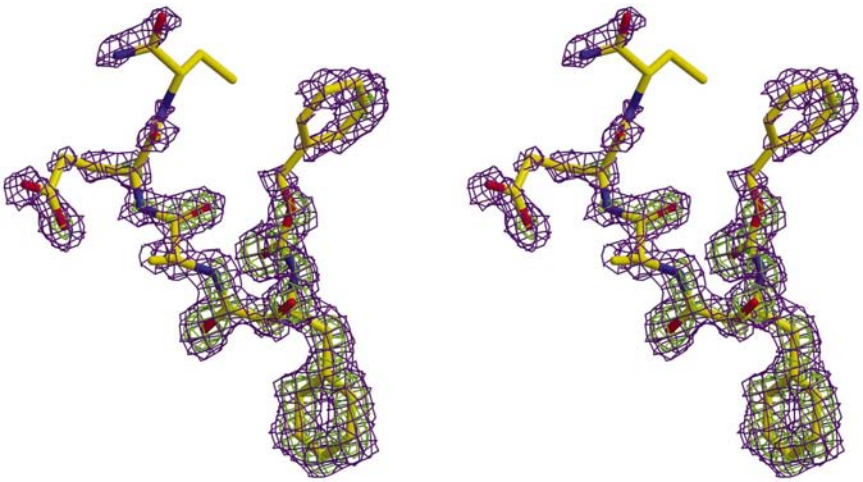

Figure 2
Inhibitor bound at the protein interface shown in an omit map (blue, 3σ level; green, 6σ level).

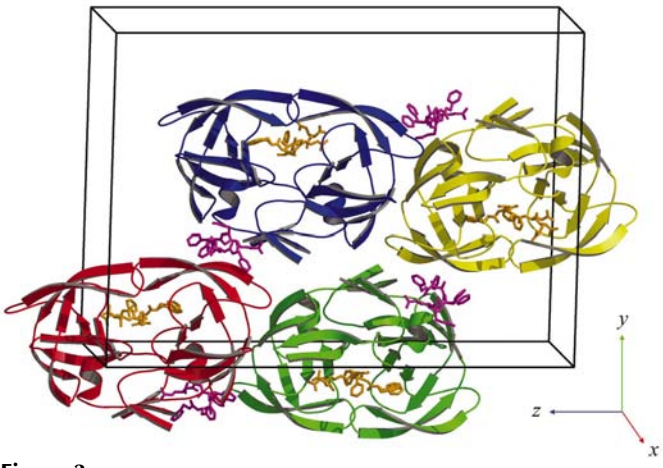

Figure 3
Crystal packing. One unit cell is shown; the orientation of its axes is marked at the bottom right. Protein molecules are represented by ribbon models coloured red for the molecule in the asymmetric part of the unit cell and coloured green, blue, and yellow for the first, second and third symmetry-related molecules, respectively. Stick models, coloured orange for the molecules bound in the active site and magenta for the molecules contacting the outer protein surface, represent the inhibitor molecules.

van der Waals interactions with all four surrounding HIV PR molecules: 35 van der Waals interactions with the dimer in the asymmetric unit (red in Fig. 4*b*), seven van der Waals interactions with a dimer in the neighbouring unit cell (yellow molecule in Fig. 4*b*), 14.5 van der Waals interactions with the dimer in the first symmetry-related position (green molecule in Fig. 4*b*) and 30 van der Waals interactions with the dimer in the second symmetry-related position (blue molecule in Fig. 4*b*).

When counted per HIV PR dimeric molecule, interactions with outer ligands comprise one hydrogen bond and 35 + 7 + 14.5 + 30 (*i.e.* a total of 86.5) van der Waals contacts.

The polypeptide chains of HIV PR in the binding regions of the outer ligand remain undistorted as revealed by direct comparison with the present hexagonal form (r.m.s.d. is 0.18 Å for the main-chain atoms) or with other HIV PR structures, *e.g.* PDB code 1hxw (Kempf *et al.*, 1995).

3.3. Inhibitor conformation: inside and outside the active site

The exclusive presence of the *R* stereoisomer in the complex (despite the presence of sufficient amounts of the *S* stereoisomer before and during crystal growth) is clearly evidenced by the omit map for the active-site molecule (Brynda *et al.*, 2004) as well as for the outer ligand, as shown in Fig. 2. The inhibitor molecule bound in the active site displays interactions of its main chain and side chains that are similar in most HIV PR complexes with peptidomimetic inhibitors, except for the phenylnorstatine moiety of the present inhibitor, which maintains a unique type of hydrogen bonding (Brynda *et al.*, 2004). The inhibitor bound to the active site displays the usual extended conformation, corresponding to its accommodation in the enzyme active site. When this conformation is superimposed on the conformation of the same compound bound as the outer ligand (Fig. 4*a*) many differences become evident. The outer ligand has a bent conformation corresponding to accommodation in the intermolecular space (Fig. 4*b*) and to the above-described interaction with the protein-surface residues. There are, however, no evident hydrogen-bonding or Coulombic interactions within the outer ligand itself that would induce its bent conformation. Three major differences in the backbone torsion angles (active site *versus* outer ligand) are C8—N10—C11—C21, −75.7° *versus* −116.2°, N10—C11—C21—C, 143.4° *versus* 74.8°, and φ Phe C—N—CA—C, −66.4° *versus* −125.4°. The same results are obtained on comparison of the outer ligand with the active-site inhibitor of the $P6_1$ form.

The inhibitor surface area buried upon binding as an outer ligand is 674 Å^2, which represents 70% of the total solvent-accessible surface area of the inhibitor in this conformation (954 Å^2).

3.4. Correlation of crystal packing and resolution limits

Inhibitor binding at the protein interface is accompanied by formation of crystals of the common $P2_12_12_1$ symmetry but with characteristic crystal packing, with an alteration in intermolecular contacts and the replacement of disordered solvent molecules. In a search for a correlation between crystal packing and resolution limits, the present orthorhombic and hexagonal structures were compared by (i) the numbers of intermolecular hydrogen bonds and van der Waals contacts per HIV PR molecule and (ii) the density of packing expressed as volume of the unit cell per HIV PR molecule (see §2) or as per cent solvent content. The latter comparison was then performed for a group of relevant PDB-deposited structures.

The present orthorhombic and hexagonal structures display similar extents of direct protein–protein interaction: 24 hydrogen bonds and 214 van der Waals contacts per HIV PR

molecule in the orthorhombic structure and 20 hydrogen bonds and 206 van der Waals contacts in the hexagonal structure. Overall intermolecular contacts are, however, augmented in the orthorhombic form compared with the hexagonal structure. The incremental interactions, comprising one hydrogen bond and 86.5 van der Waals contacts per HIV PR molecule, are described in more detail in §3.2. The difference between the overall intermolecular interactions in the orthorhombic and hexagonal forms is thus substantial (300.5 van der Waals contacts *versus* 214 van der Waals contacts) and the protein–ligand–protein interactions can be appreciated as a factor contributing to the strength of the crystal network and which probably improves the practical diffraction quality.

The outer-ligand-containing orthorhombic form displays very dense crystal packing: its per HIV PR molecule volume, 44 815.5 Å^3, is the fourth smallest value among the 168 PDB-deposited structures of HIV-1 PR complexes and its solvent content, 36.1%, is the lowest. However, the importance of the dense crystal packing cannot simply be inferred since the hexagonal form is packed with a similarly high density (43 771.9 Å^3, the smallest value of the 168 structures, and 36.7%, the second lowest solvent content). Also, the overall ranking of the 168 structures according to their density of crystal packing (data not shown) gives no obvious clues. Contribution of the density of packing to the crystal quality becomes apparent with a correlation performed separately for structures of $P2_12_12_1$ symmetry (55 PDB entries, when not including another three of >59 000 Å^3 per HIV PR molecule volume). The plot of the calculated 'per HIV PR molecule volumes' and the stated resolution limits (Fig. 5) displays a direct proportionality trend for this group, although with a mediocre correlation coefficient of 0.498. In qualitative terms, this correlation can probably be understood as the crystal quality being improved with denser crystal packing since the protein molecules are less exposed to solvent and their side chains are more restricted in movement.

4. Discussion

Several aspects of the binding of a novel compound Z-Pns-Phe-Glu-Glu-NH_2 to HIV protease have already been examined at the level of an atomic resolution complex structure (Brynda *et al.*, 2004). The central part of this compound includes the pseudodipeptide phenylnorstatine-phenylalanine (Pns-Phe), which has an extended five-atom-long backbone between two key aromatic groups (Pns C11–Phe C^{α}) and resembles successful Pns-Pro-based inhibitors (Reiling *et al.*, 2002).

A second molecule of inhibitor, bound as an outer ligand, makes contacts with functionally important regions of the enzyme, *i.e.* with the flap structure that moves in each turn of the catalytic cycle and with the Trp6 residue in the amino-terminal region of the polypeptide chain involved in the obligatory dimerization of the enzyme subunits (Figs. 3 and 4*b*). Nevertheless, at least two arguments exist against the consideration of an inhibitory role of the outer ligand molecule. Firstly, assembly in solution of a complex consisting of five components (four protein molecules and one ligand molecule, as in the crystal) seems unlikely. Secondly, the protein regions in contact with the ligand are of undistorted conformations and this contrasts with known mechanisms of

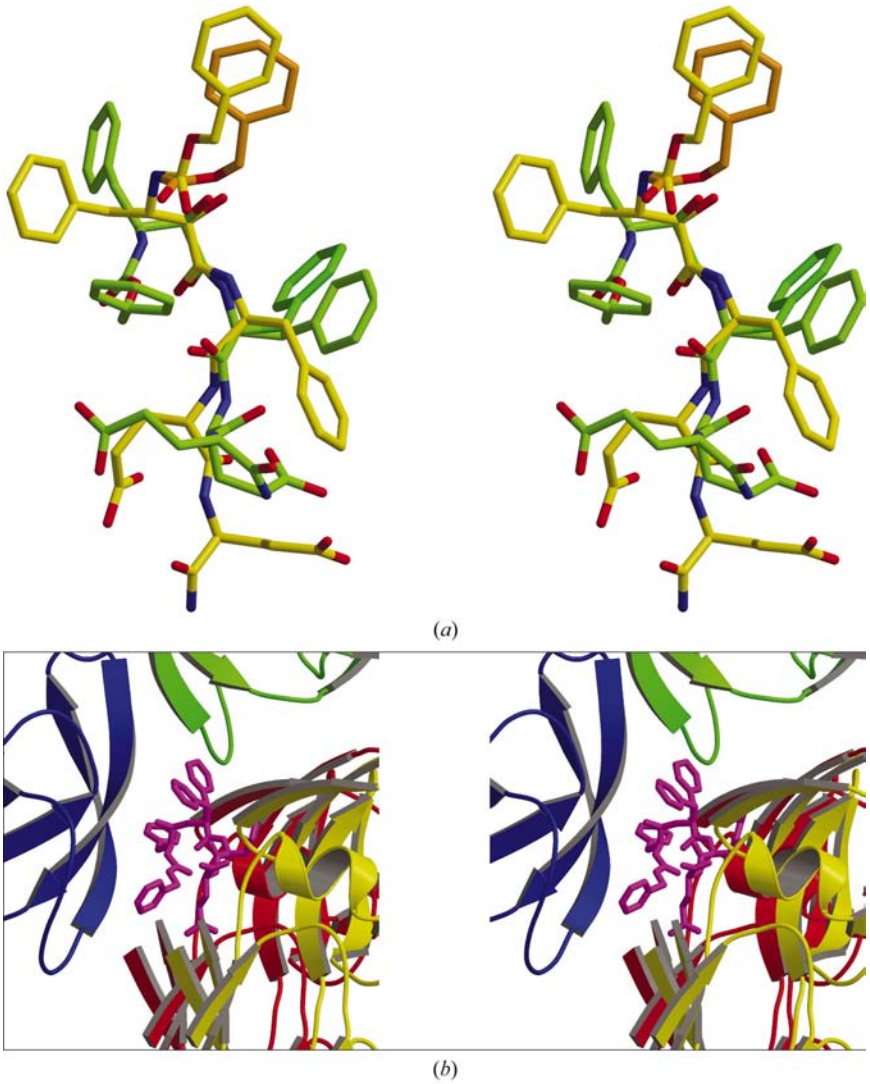

Figure 4
Details and comparisons of the ligand structures. (*a*) Stereoview comparison of the conformations of the active-site inhibitor (yellow) and the outer ligand (green). (*b*) Stereoview of inhibitor (magenta) maintaining contacts with four protein molecules: red colour corresponds to the protein molecule in the asymmetric part of unit cell and yellow shows that in the neighbouring cell; green corresponds to the third symmetric position and blue to the fourth symmetric position.

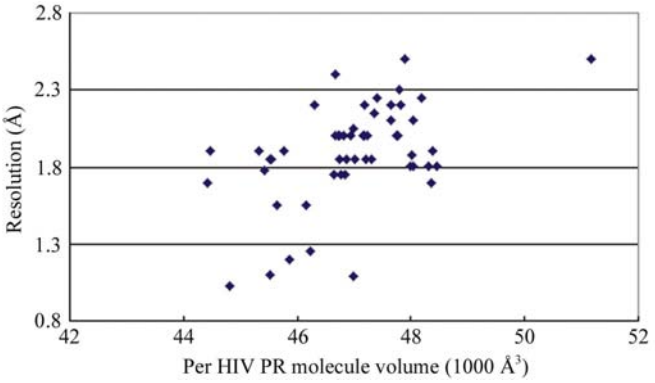

Figure 5
Plot of the calculated 'per HIV PR molecule volumes' and the stated resolution limits for 55 PDB entries. For details, see text.

HIV PR inhibition outside its active side: the inhibitory antibodies with epitopes in the flap or in the amino-terminal HIV PR region do substantially distort the epitope peptide conformations (Lescar *et al.*, 1997; Rezacova *et al.*, 2001).

The quality of a protein crystal is defined by its shape, size, mosaicity and resolution limit (McPherson, 1998). Very generally, resolution limit is determined by the order of the crystal structure: a highly ordered crystal will have a high resolution limit. While negative influences, such as presence of chemical or conformational heterogeneities, are easily understandable, positive factors improving crystal resolution limit often lack rigorous explanation. In literature, factors that facilitate initial crystal growth, improve crystal quality or expand resolution limit are frequently discussed together, as in the case of metal ions, additives or detergents. An additional inhibitor molecule bound at the protein interface has never been found in the large variety of HIV PR crystal structures solved before and described cases of the improvement achieved by co-crystallization with a specific ligand (*e.g.* Trakhanov *et al.*, 1998) do not bear sufficient analogy to the present case. We believe that two conclusions may be drawn, fully based on the above experimental results. Firstly, improvement of the resolution evidently arises from the characteristic crystal packing in view of the substantial difference between the diffraction of the orthorhombic crystals containing the outer ligand and that of the conventional hexagonal ones. Second, all quantitative parameters match the criteria for supplementary ordering of the crystal with the interface ligand binding: the movement of protein molecules relative to each other may become restricted owing to stronger networking and the movement of side chains may be restricted in larger areas of the protein molecules owing to replacement of disordered solvent.

This work was supported by the project No. K5011112 awarded by the Academy of Sciences of the Czech Republic, by grants from the Grant Agency of the Czech Republic (203/98/K023 and 203/020405), a grant from the Ministry of Public Health (NI/6339-3) and by a grant from the 5th Framework of the European Commission (QLK2-CT-2001-02360).

References

Brynda, J., Rezáčová, P., Fábry, M., Horejsi, M., Štouračová, R., Sedláček, J., Souček, M., Hradílek, M., Lepsik, M. & Konvalinka, J. (2004). *J. Med. Chem.* **47**, 2030–2036.
Collaborative Computational Project, Number 4 (1994). *Acta Cryst.* D**50**, 760–763.
Dohnálek, J., Hašek, J., Dušková, J., Petroková, H., Hradílek, M., Souček, M., Konvalinka, J., Brynda, J., Sedláček, J. & Fábry, M. (2001). *Acta Cryst.* D**57**, 472–476.
Erickson, J. W. & Burt, S. K. (1996). *Annu. Rev. Pharmacol. Toxicol.* **36**, 545–571.
Houghten, R. A., Pinilla, C., Blondelle, S. E., Appel, J. R., Dooley, C. T. & Cuervo, J. H. (1991). *Nature (London)*, **354**, 84–86.
Kabsch, W. (2001*a*). *International Tables for Crystallography*, Vol. *F*, edited by M. G. Rossmann & E. Arnold, pp. 730–734. Dordrecht: Kluwer Academic Publishers.
Kabsch, W. (2001*b*). *International Tables for Crystallography*, Vol. *F*, edited by M. G. Rossmann & E. Arnold, pp. 218–224. Dordrecht: Kluwer Academic Publishers.
Kempf, D. J. *et al.* (1995). *Proc. Natl Acad. Sci. USA*, **92**, 2484–2488.
King, N. M., Melnick, L., Prabu-Jeyabalan, M., Nalivaika, E. A., Yang, S. S., Gao, Y., Nie, X., Zepp, C., Heefner, D. L. & Schiffer, C. A. (2002). *Protein Sci.* **11**, 418–429.
Lescar, J., Štouračová, R., Riottot, M.-M., Chitarra, V., Brynda, J., Fábry, M., Horejsi, M., Sedláček, J. & Bentley, G. A. (1997). *J. Mol. Biol.* **267**, 1207–1222.
McPherson, A. (1998). *Crystallization of Biological Macromolecules.* Cold Spring Harbor: Cold Spring Harbor Laboratory Press.
McRee, D. E. (1999). *J. Struct. Biol.* **125**, 156–165.
Mahalingam, B., Boross, P., Wang, Y.-F., Louis, J. M., Fischer, C. C., Tozser, J., Harrison, R. W. & Weber, I. T. (2002). *Proteins Struct. Funct. Genet.* **48**, 107–116.
Mahalingam, B., Louis, J. M., Hung, J., Harrison, R. W. & Weber, I. T. (2001). *Proteins Struct. Funct. Genet.* **43**, 455–464.
March, D. R., Abbenante, G., Bergman, D. A., Brinkworth, R. I., Wickramasinghe, W., Begun, J., Martin, J. L. & Fairlie, D. P. (1996). *J. Am. Chem. Soc.* **118**, 3375–3379.
Prabu-Jeyabalan, M., Nalivaika, E. & Schiffer, C. A. (2000). *J. Mol. Biol.* **301**, 1207–1220.
Reiling, K. K., Endres, N. F., Dauber, D. S., Craik, C. S. & Stroud, R. M. (2002). *Biochemistry*, **41**, 4582–4594.
Řezáčová, P., Lescar, J., Brynda, J., Fábry, M., Horejsi, M., Sedláček, J. & Bentley, G. A. (2001). *Structure*, **9**, 887–95.
Rinnova, M., Hradílek, M., Barinka, C., Weber, J., Souček, M., Vondrasek, J., Klimkait, T. & Konvalinka, J. (2000). *Arch. Biochem. Biophys.* **382**, 22–30.
Sedláček, J., Fábry, M., Horejsi, M., Brynda, J., Luftig, R. B. & Majer, P. (1993). *Anal. Biochem.* **215**, 306–309.
Trakhanov, S., Kreimer, D. I., Parkin, S., Ames, G. F. & Rupp, B. (1998). *Protein Sci.* **7**, 600–604.
Wlodawer, A., Li, M., Gustchina, A., Dauter, Z., Uchida, K., Oyama, H., Goldfarb, N. E., Dunn, B. M. & Oda, K. (2001). *Biochemistry*, **40**, 15602–15611.
Wlodawer, A. & Vondrasek, J. (1998). *Annu. Rev. Biophys. Biomol. Struct.* **27**, 249–284.